Elasticity and Response in Nearly Isostatic Periodic Lattices

Anton Souslov, Andrea J. Liu and T. C. Lubensky[1]

[1]*Department of Physics and Astronomy, University of Pennsylvania, Philadelphia, PA 19104, USA*

(Dated: November 13, 2009)

The square and kagome lattices with nearest neighbor springs of spring constant k are isostatic with a number of zero-frequency modes that scale with their perimeter. We analytically study the approach to this isostatic limit as the spring constant k' for next-nearest-neighbor bonds vanishes. We identify a characteristic frequency $\omega^* \sim \sqrt{k'}$ and length $l^* \sim \sqrt{k/k'}$ for both lattices. The shear modulus $C_{44} = k'$ of the square lattice vanishes with k', but that for the kagome lattice does not.

PACS numbers: 63.70.+h, 83.80.Fg, 64.70.kj, 63.20.D-

An argument advanced by Maxwell [1] states that rigid assemblies of loose particles must have at least $Z_{\rm iso} = 2n_f$ contacts per particle, where n_f is the number of relevant degrees of freedom per particle. This result has been applied to many systems [2, 3], including network glasses[4, 5], rigidity percolation [6, 7], β-cristobalite [8], granular media [9, 10], protein folding [11], and elasticity in networks of semi-flexible polymers [12].

Zero-temperature packings of particles can exhibit transitions with increasing particle density from an unjammed, disordered state with no inter-particle contacts to a jammed, disordered state with an average of Z_c contacts per particle. These transitions are discontinuous because the coordination number Z_c must satisfy Maxwell's inequality. For the special case of frictionless spheres, the coordination number at the jamming transition, Z_c, appears to be exactly the minimal, or *isostatic*, value needed for mechanical stability, $Z_{\rm iso}$ [13, 14, 15]. The coincidence of the jamming transition with the threshold for mechanical stability gives rise to special properties at the transition: the coordination number Z jumps discontinuously but as the transition is approached from the high-density side, the shear modulus vanishes and length and time scales diverge as power laws [13, 14, 15, 16]. In addition, the vibrational properties just above the transition are very different from those of typical solids [3, 16, 17, 18, 19].

The behavior of the isostatic jamming transition invites comparison to second-order structural transitions, in which the vanishing of an elastic constant in an isostatic lattice signals the instability towards a shape distortion. Jamming involves a transition between two disordered states, while critical structural transitions involve a crystalline state. This raises the question of which aspects of the jamming transition apply to *all* systems, periodic or disordered, near isostatic transitions and which do not. To answer these questions, it is important to study models for which results can be rigourously established via analytic calculations. In this paper, we test the robustness of the connection between isostaticity, power-law elastic moduli and vibrational properties by an exact analytical exploration of the approach to the threshold of mechanical stability in fully periodic, nearly isostatic systems. Specifically, we study two lattices, the $2D$ square and kagome lattices, shown in Fig. 1, with nearest-neighbor (NN) harmonic springs of spring constant k and next-nearest-neighbor (NNN) harmonic springs with spring constant k'. The isostatic structural transition is then approached continuously as $k' \to 0$ since both systems are isostatic there with $Z_c = 4$. To describe the phase that results when $k' < 0$, it is necessary to add a nonlinear term gx^4 to the energy [20].

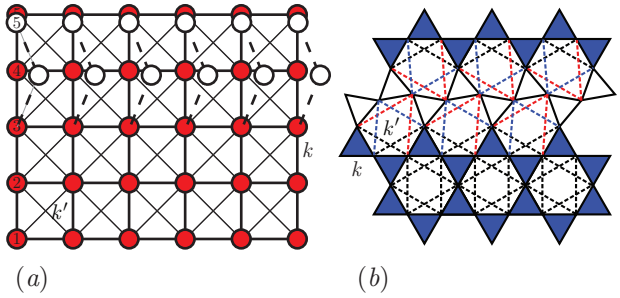

FIG. 1: (Color Online) (a) Square and (b) kagome lattices with NN springs of spring-constant k and NNN springs of spring constant k'. White circles in (a) and white triangles in (b) show a zero-energy distortion.

Our principal results are that in both the square and kagome lattices, there is a characteristic frequency $\omega^* \sim \sqrt{k'}$ and a length $l^* \sim \sqrt{k/k'}$ that follow directly form the form of the wavenumber- and frequency-dependent response function but that can also be obtained from cutting arguments [3, 16]. However, the shear modulus exponent is different in the three systems, showing that isostaticity does not confer universality on all power-law properties near the transition.

It is useful first to understand the two states that straddle the structural transition. Above the transition, where $k' > 0$, the square/kagome lattice is stable. Below the transition, where $k' < 0$ (and $g > 0$), the N_0 zero modes at $k' = 0$ develop positive or negative amplitudes, and there are $\sim a^{N_0}$, where $a > 1$, distinct ground states. In this paper, we will restrict our attention to the case $k' \geq 0$, and we will use the harmonic approximation.

Now consider the square lattice shown in Fig. 1(a) with NNN nonlinear springs. This lattice has $N = N_x N_y$ sites and $N_{nn} = 2N_x N_y - N_x - N_y$ nearest-neighbor

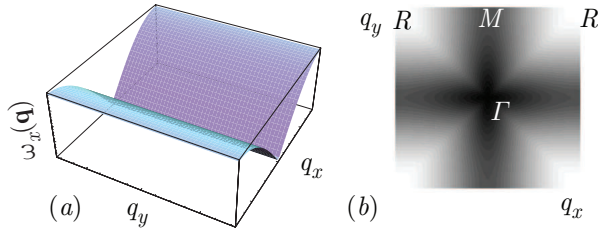

FIG. 2: (a) $\omega_x(\mathbf{q})$ when $k' = 0$ showing the line of zero energy at $q_x = 0$ and one-dimensional dispersion as a function of q_x at fixed q_y. (b) Density plot of the low-energy phonon mode when $k' = 0.02k$ showing $\cos 4\theta$ modulation at small $\mathbf{q}$ and one-dimensional isostatic behavior at large $\mathbf{q}$.

bonds. Thus when $k' = 0$, this system is isostatic with a number of zero-frequency modes, $N_0 = 2N - N_{nn} = N_x + N_y$, equal to half the perimeter of the system. When $k' > 0$, these modes become quasi-isostatic with nonzero frequencies that vanish as $k' \to 0$. The components of the dynamical matrix are easily calculated [21]

$$\begin{aligned} D_{xx}(\mathbf{q}) &= D_{yy}(q_y, q_x) = 4k\sin^2(q_x/2) + 4k'\sin^2(q_y/2) \\ &+ 4k'\sin^2(q_x/2) - 8k'\sin^2(q_x/2)\sin^2(q_y/2) \\ D_{xy}(\mathbf{q}) &= D_{yx}(\mathbf{q}) = 2k'\sin(q_x)\sin(q_y), \end{aligned} \tag{1}$$

where we set the lattice constant a equal to 1. In the continuum limit $q \ll 1$, $D_{ij}(\mathbf{q})$ obtains the form dictated by elasticity theory with elastic constants $C_{11} = C_{xxxx} = C_{yyyy}$, $C_{12} = C_{xxyy}$ and $C_{44} = C_{xyxy}$: [21]

$$\begin{aligned} &D_{xx}(\mathbf{q}) = C_{11}q_x^2 + C_{44}q_y^2;\ \ D_{yy}(\mathbf{q}) = C_{11}q_y^2 + C_{44}q_x^2 \\ &D_{xy}(\mathbf{q}) = (C_{12} + C_{44})q_x q_y, \end{aligned} \tag{2}$$

and we can relate k and k' to the elastic constants: $C_{11} = k + k'$, $C_{44} = C_{12} = k'$. Thus, the shear modulus vanishes as $k' \to 0$. When $k' = 0$, $D_{ij}(\mathbf{q})$ breaks up into two independent one-dimensional compressional phonon systems: it is diagonal with $D_{xx}(\mathbf{q}) = 4k\sin^2(q_x/2)$ independent of q_y and $D_{yy}(\mathbf{q}) = 4k'\sin^2(q_y/2)$ independent of q_x. Thus at $q_x = 0$, $D_{xx}(\mathbf{q})$ vanishes for all points along the line $-\pi < q_y < \pi$. Note that at a standard structural phase transition, components of $D_{ij}(\mathbf{q})$ vanish at one or possibly a discrete set of points in the Brillouin Zone (BZ) when an elastic modulus vanishes. In contrast, for the periodic isostatic system, components of $D_{ij}(\mathbf{q})$ vanish along lines.

The one-dimensional nature of $D_{ij}(\mathbf{q})$ gives rise to compressional phonons with frequencies $\omega_{x,y}(\mathbf{q}) = 2\sqrt{k'}|\sin q_{x,y}/2|$ [Fig. 2(a)] and a one-dimensional density of states $\rho(\omega)(2/\pi)/\sqrt{4k - \omega^2}$ with a nonzero value $\rho_0 = (\pi\sqrt{k})^{-1}$ at $\omega = 0$ as shown in Fig. 3(a).

When $k' > 0$, modes exhibit a $\cos 4\theta$ modulation at low frequency and one-dimensional isostatic behavior at larger $\mathbf{q}$ [Fig. 2(b)]. When $0 < k' \ll k$, $D_{ij}(\mathbf{q})$ is well approximated as a diagonal matrix with $D_{xx}(\mathbf{q}) = kq_x^2 + 4k'\sin^2(q_y/2)$ with associated eigenfrequency $\omega_x(\mathbf{q}) \sim \sqrt{D_{xx}(\mathbf{q})}$. These expressions immediately define a characteristic frequency

$$\omega^* = 2\sqrt{k'} \tag{3}$$

as the frequency at the point $M = (0, \pi)$ on the BZ edge. The first term in $D_{xx}(\mathbf{q})$ represents the long-wavelength anomalous *isostatic (iso)* modes that are present when $k' = 0$, whereas the second represents the effects of NNN coupling. When $q_x = 0$, the only length scale in the problem is the unit lattice spacing, and no divergent length scale can be extracted from $D_{xx}(0, q_y)$ as it can be in the case of the structural phase transition. When the first term is large compared to the second, $D_{xx}(\mathbf{q})$ reduces to its form for the isostatic $k' = 0$ limit, and we can extract a length by comparing these two terms. The shortest length we can extract comes from comparing kq_x^2 to $D_{xx}(\mathbf{q})$ at point M on the zone edge, i.e.

$$l^* = (1/2)\sqrt{k/k'} \equiv 1/q^*. \tag{4}$$

If $q_y < \pi$, the isostatic limit is reached when $q_x > q^*$. A similar analysis applies to $D_{yy}(\mathbf{q})$ when $q_y > q^*$. If a square of length l is cut from the bulk, the wavenumbers of its excitations will be greater than π/l, and for $ql^* > 1$, all modes within the box will be effectively isostatic ones. This construction is equivalent to the cutting argument of Wyart et al. [3, 22].

Equation (4) is identical to the length at which the frequency of the compressional mode $\omega_x(q_x, 0) = \sqrt{k}/l^* \sim \sqrt{C_{11}}/l^*$ becomes equal to ω^*. A meaningful length from the transverse mode $\omega_x(0, q_y)$ cannot be extracted in a similar fashion. The full phonon spectrum [Fig. 3(a)] exhibits acoustic phonons identical to those of a standard square lattice at $q \ll 1$ and a saddle point at the point M. Thus, the low-frequency density of states is Debye-like: $\rho(\omega) = (\omega/(2\pi))/\sqrt{kk'}$ with a denominator that, because of the anisotropy of the square lattice, is proportional to the geometric mean of longitudinal and transverse sound velocities rather than to a single velocity. In addition $\rho(\omega)$ exhibits a logarithmic van Hove singularity at ω^* and approaches the one-dimensional limit $(1/\pi)/\sqrt{k}$ at $\omega^* \ll \omega \ll 2\sqrt{k}$. The frequency ω^* [Eq. (3)] is recovered by equating the low-frequency Debye form at ω^* to the high-frequency isostatic form of the density of states.

The kagome lattice can be viewed as an array of one-dimensional staggered linear rows, parallel to the x-axis, of pairs of opposing triangles as shown in Fig. 1. Identical arrays with rows parallel to $(\cos 2\pi/3, \pm\sin 2\pi/3)$ can be identified. As in the square lattice, each site has $2d = 4$ nearest neighbors in the bulk. A counting procedure similar to that used for the square lattice yields N_0 proportional to the $\sqrt{N}$ for lattice of N sites.

The isostatic (iso) modes correspond to identical rotations about their top vertices of all of the "up" pointing triangles in any row in the horizontal (or symmetry-equivalent) grid. These rotations require counter rotations of connected "down" pointing triangles as shown in Fig. 1(b). There are three sites per unit cell (which

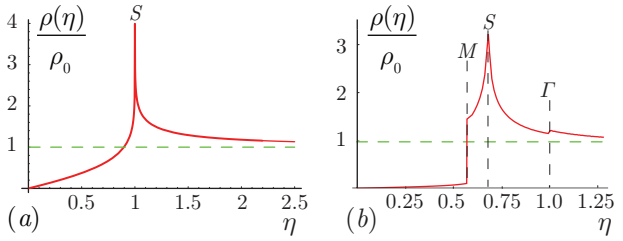

FIG. 3: (Color Online) Density of states as a function of $\eta = \omega/\omega^*$ for (a) the square and (b) kagome lattices, showing their constant value when $k' = 0$ (dashed green line) and van Hove singularities, from the saddle at S and minima at M and Γ, whose frequencies all scale as $\omega^* \propto \sqrt{k'}$ when $k' > 0$.

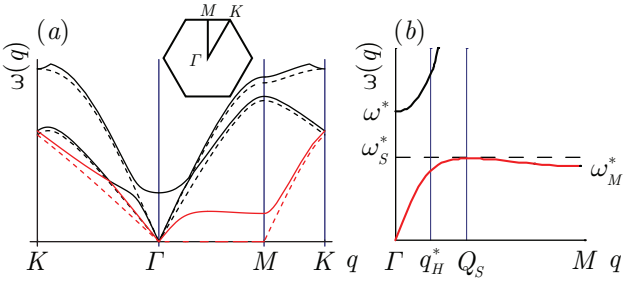

FIG. 4: (Color Online) (a) Phonon dispersion along symmetry directions. The dotted lines are for $k' = 0$ and the solid lines are for $k' = 0.02$. The isostatic and quasi-isostatic branches are in red. (b) shows isostatic and shear modes along ΓM and indicates characteristic frequencies and wavenumbers.

we take to be those in the "up" triangles) in the kagome lattice and six phonon branches [Fig. 4(a)]. Three of these are high-energy optical branches, two are acoustic and one is isostatic. The zero modes of the latter show up as three lines of zero frequency along $q_x = 0$ [$\Gamma = (0,0)$ to $M = (0, G_0/2)$, where $G_0 = 4\pi/\sqrt{3}$, in the BZ] and the two symmetry-related lines as shown in Fig. 5(a). Away from $q_x = 0$, the isostatic mode frequency is $\omega_I(\mathbf{q}) = c_x q_x$, where $c_x = \sqrt{3k}/4$ for small q_x. This behavior is identical to that of the square lattice. The resulting density of states decreases linearly with ω from a nonzero value $\rho_0 = 3G_0/(4\pi^2 c_x) = 8/(\pi\sqrt{k})$ at $\omega = 0$. The total low-frequency density of states from the two acoustic modes and the isostatic mode is independent of ω and equal to ρ_0 at small ω [Fig. 3(b)].

When springs of spring constant k' are added to the NNN bonds shown in Fig. 1(b), the quasi-isostatic mode along $q_x = 0$ [Fig. 4(b)] has nonzero frequency of order $\sqrt{k'}$ for all $q_y > 0$ and gives rise to various lengths of order $l^* \sim \sqrt{k/k'}$. At $q_x = 0$ and low values of q_y, this mode hybridizes with the transverse phonon mode to produce a gapped translation-rotation mode with frequency

$$\omega^* = \sqrt{6k'} \tag{5}$$

at $\mathbf{q} = 0$. At small $\mathbf{q}$, there are isotropic longitudinal and transverse sound modes with respective velocities $c_L = \sqrt{3k}/4$ and $c_T = \sqrt{k}/4$. The lowest frequency mode after hybridization at $q_x = 0$ is a transverse phonon near $q_y = 0$ and predominantly an isostatic rotation mode at $q_y > q_H^*$, where $q_H^* = 4\sqrt{3k'/k} \equiv 1/l_H^*$ can be termed a hybridization wave number. This mode reaches a maximum frequency $\omega_S^* = \omega^*/\sqrt{2}$ at a saddle point at $q_y = Q_S = 4(3k'/2k)^{1/4} \sim (l^*)^{-1/2}$ and a local minimum with frequency $\omega_M^* = \omega^*/\sqrt{3}$ at the zone-edge point M. At low frequency, the DOS is Debye-like: $\rho(\omega) = (\omega/2\pi)(c_L^{-2} + c_T^{-2}) = 32\omega/(2\pi k)$. The points M, Γ and $S = (0, Q_S)$ give rise to van Hove singularities in the DOS. The minimum point M produces a jump $\Delta\rho_M = 8\sqrt{2}/\pi\sqrt{k} > \rho_0$ at ω_M^*, the saddle S produces a logarithmic singularity at ω_S^*, and the minimum at Γ a jump $\Delta\rho_\Gamma = (16/\pi)\sqrt{3k'/2k} \ll \rho_0$, which is just visible in Fig. 3(b).

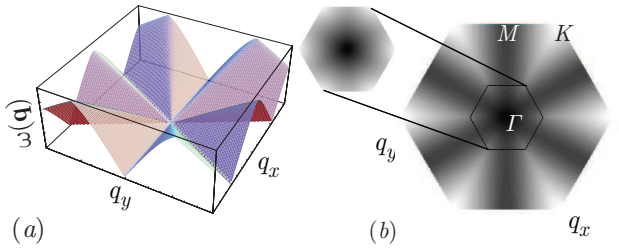

FIG. 5: (a) Plot of iso mode at $k' = 0$. (b) density plot of iso mode at $k' = 0.02k$. Inset: circular symmetry at origin.

Lengths that scale as $\sqrt{k/k'}$ can be introduced in much the same way as in the square lattice. The square of the low-frequency isostatic-shear mode at $q_x = 0$ increases as $c_x^2 q_x^2$ for nonzero shear, and lengths $l_S^* = (1/4)\sqrt{k/k'}$ and $l_M^* = (\sqrt{6}/8)\sqrt{k/k'}$ follow from comparing $c_x q_x$ to ω_S^* and ω_M^*, respectively. These two lengths are longer than the hybridization length, l_H^*. Thus, it is only at length scales less than l_H^* that isostatic modes are retrieved completely, and we should take

$$l^* = l_H^* = (1/4)\sqrt{k/(3k')}. \tag{6}$$

The less divergent length $\xi_S = Q_S^{-1} \sim \sqrt{l^*}$ determines the position of the saddle S and does not describe the same physics as the other lengths.

The long-wavelength, low-frequency properties of the kagome lattice are best understood by considering the effective low-energy dynamical matrix $\tilde{D}_{ij}$ obtained by integrating out the high-energy modes. This matrix is conveniently represented in a basis consisting of the longitudinal (L) and transverse (T) phonons and the mixed rotation-translation gapped mode (η) at $\mathbf{q}$: $\tilde{D}_{LT} = \tilde{D}_{TL} = 0$, and components are

$$\begin{aligned} \tilde{D}_{LL} &= 3kq^2/16;\ \tilde{D}_{TT} = kq^2/16;\ \tilde{D}_{\eta\eta} = 6k' + kq^2/16 \\ \tilde{D}_{L\eta} &= \tilde{D}^*_{\eta L} = kq^2\cos(3\theta)/16 \\ \tilde{D}_{T\eta} &= \tilde{D}^*_{\eta T} = -i(\sqrt{3}/2)k'q + kq^2\sin(3\theta)/16, \end{aligned} \tag{7}$$

where θ is the angle that $\mathbf{q}$ makes with the x-axis. When $k' = 0$, the transverse phonon and rotation-translation

TABLE I: Frequencies, lengths, and elastic moduli in square and kagome lattices and the marginally-jammed (MJ) state of disordered sphere packings. ω^*, l^* and B scale the same way in all lattices if we take $k' \sim (\Delta z)^2$, but G does not.

Quantity	Square	Kagome	MJ
l^*	$\left(\frac{k}{k'}\right)^{1/2}$	$\left(\frac{k}{k'}\right)^{1/2}$	$(\Delta z)^{-1}$
ω^*	$(k')^{1/2}$	$(k')^{1/2}$	$(\Delta z)^1$
G	k'	k	$(\Delta z)^1$
B	k	k	$(\Delta z)^0$

mode mix at $q_x = 0$ ($\theta = \pi/2$) to produce the zero isostatic rotation mode and a sound mode with $\omega = \sqrt{k/8}q_y$. In addition, there is the longitudinal mode with $\omega = (\sqrt{3k}/4)q_y$. When $k' \neq 0$, the off-diagonal terms can be ignored to lowest order in $\mathbf{q}$, leading to longitudinal and transverse sound modes with respective velocities $c_L = \sqrt{B}$ and $c_T = \sqrt{G}$, arising from bulk and shear moduli $B = 3k/16$ and $G = k/16$. Note that the shear modulus is proportional to k; this is in contrast to the square lattice where $G \propto k'$. To understand how this comes about, it is instructive to look at the TT component of the phonon susceptibility,

$$\chi_{TT}(q,\theta) = D^{-1}_{TT}(q,\theta) = \frac{16}{kq^2}\frac{6 + (ql^*)^2(3 - \cos^2 3\theta)}{6 + 2(ql^*)^2\cos^2 3\theta}. \quad (8)$$

When $ql^* \ll 1$, this reduces to the required isotropic form $1/(Gq^2)$. When $ql^* \gg 1$, χ_{TT} is anisotropic with value $1/(Gq^2)$ for $\cos 3\theta = 1$ and $1/(6k')$ for $\cos 3\theta = 0$.

We can now compare the properties of nearly isostatic lattices with those of disordered sphere packings. Marginally-jammed packings with volume fraction $\phi \equiv \phi_c + \Delta\phi$, just above the volume fraction ϕ_c at the jamming threshold, have an average number of contacts per sphere $z \equiv z_c + \Delta z$, where $z_c = 2d$, and $\Delta z \sim (\Delta\phi)^{1/2}$ [13, 15]. They are macroscopically isotropic with bulk and shear moduli that for harmonic inter-particle potentials scale respectively as $B \sim (\Delta z)^0$ and $G \sim (\Delta z)^1$ [13, 15]. The longitudinal and transverse sound velocities then scale as $c_L \sim (\Delta z)^0$ and $c_T \sim (\Delta z)^{1/2}$. The density of states has a plateau above a frequency ω^* [15, 16]. A length scale $l^* \sim 1/\Delta z$ can be extracted by equating c_L/l^* to ω^* [16], or from the response to a point perturbation [23]. This scaling emerges from the cutting arguments of Refs. 3, 17. A second length $l^*_T \sim (\Delta z)^{-1/2}$ can be defined from $c_T/l^*_T = \omega^*$ [16] and is important for energy transport [19].

The most robust features are the scalings of $\omega^* \sim \sqrt{k'}$ and $l^* \sim 1/\sqrt{k'}$ in both the square and kagome lattices. Effective medium calculations [24] for these lattices with NNN bonds added with probability $P \sim \Delta z$ yield $k' \sim (\Delta z)^2$; this correspondence yields the observed scalings of ω^* and l^* for marginally-jammed systems. These scalings are likely to be robust for all nearly-isostatic systems. However, the power-law scaling of the shear modulus is not universal (Table I). The shear moduli of marginally-jammed systems and the square lattice both vanish with Δz (with different powers), but G of the kagome lattice is proportional to k and does not vanish. Thus, different isostatic transitions can fall into different universality classes. This conclusion is consistent with recent numerical results for disordered systems near isostaticity, which show different scalings of bulk moduli [26].

We thank NSF-DMR-0520020 (AS), NSF-DMR-0804900 (TCL), and DE-FG02-05ER46199 (AJL).

[1] J. C. Maxwell, Philosophical Magazine **27**, 294 (1865).
[2] S. Alexander, Physics Rep. **296**, 65 (1998).
[3] M. Wyart, Annales De Physique **30**, 1 (2005).
[4] J. C. Phillips, J. of Non-Cryst. Solids **43**, 37 (1981).
[5] M. F. Thorpe, J. of Non-Cryst. Solids **57**, 355 (1983).
[6] D. J. Jacobs and M. F. Thorpe, Phys. Rev. Lett. **75**, 4051 (1995).
[7] P. M. Duxbury *et al.*, Physical Review E **59**, 2084 (1999).
[8] I. P. Swainson and M. T. Dove, Phys. Rev. Lett. **71**, 193 (1993); **71**, 3610 (1993).
[9] S. F. Edwards and D. V. Grinev, Phys. Rev. Lett. **82**, 5397 (1999).
[10] A. V. Tkachenko and T. A. Witten, Phys. Rev. E **60**, 687 (1999).
[11] A. J. Rader *et al.*, Proc. Nat. Acad. Sci. **99**,3540 (2002).
[12] C. Heussinger, B. Schaefer, and E. Frey, Phys. Rev. E **76**, 031906 (2007).
[13] D. J. Durian, Phys. Rev. Lett. **75**, 4780 (1995).
[14] C. S. O'Hern *et al.*, Phys. Rev. Lett. **88**, 075507 (2002).
[15] C. S. O'Hern *et al.*, Phys, Rev. E **68**, 011306 (2003).
[16] L. E. Silbert, A. J. Liu, and S. R. Nagel, Phys. Rev. Lett. **95**, 098301 (2005).
[17] M. Wyart, S. R. Nagel, and T. A. Witten, Europhys. Lett. **72**, 486 (2005).
[18] N. Xu, *et al.*, Phys. Rev. Lett. **98**, 175502 (2007).
[19] N. Xu, *et al.*, Phys. Rev. Letters **102**, 038001 (2009).
[20] A. Souslov and T.C. Lubensky (unpublished)
[21] N. W. Ashcroft and N.D. Mermin, Solid State Physics (Hold, Rinehart and Winston, New York, 1976)
[22] M. Wyart, *et al.*, Phys. Rev. E **72**, 051306 (2005).
[23] W. G. Ellenbroek *et al.*, Phys. Rev. Lett. **97**, 258001 (2006).
[24] X. Mao and T. Lubensky, Unpublished (2009).
[25] N. Xu, V. Vitelli, A. J. Liu and S. R. Nagel, unpublished.
[26] W. G. Ellenbroek, Z. Zeravcic, W. van Saarloos and M. van Hecke, arXiv:0907.0012 (2009).